ACS central science

Research Article

http://pubs.acs.org/journal/acscii

"Zipped Synthesis" by Cross-Metathesis Provides a Cystathionine β-Synthase Inhibitor that Attenuates Cellular H_2S Levels and Reduces Neuronal Infarction in a Rat Ischemic Stroke Model

Christopher D. McCune,[†] Su Jing Chan,[‡] Matthew L. Beio,[†] Weijun Shen,[†] Woo Jin Chung,[†] Laura M. Szczesniak,[†] Chou Chai,[§] Shu Qing Koh,[‡] Peter T.-H. Wong,*[,‡] and David B. Berkowitz*[,†]

[†]Department of Chemistry, University of Nebraska, Lincoln, Nebraska 68588, United States

[‡]Department of Pharmacology, Yong Loo Lin School of Medicine, National University of Singapore, Singapore 117597

[§]Neurodegeneration Research Laboratory, National Neuroscience Institute, Singapore 308433

Supporting Information

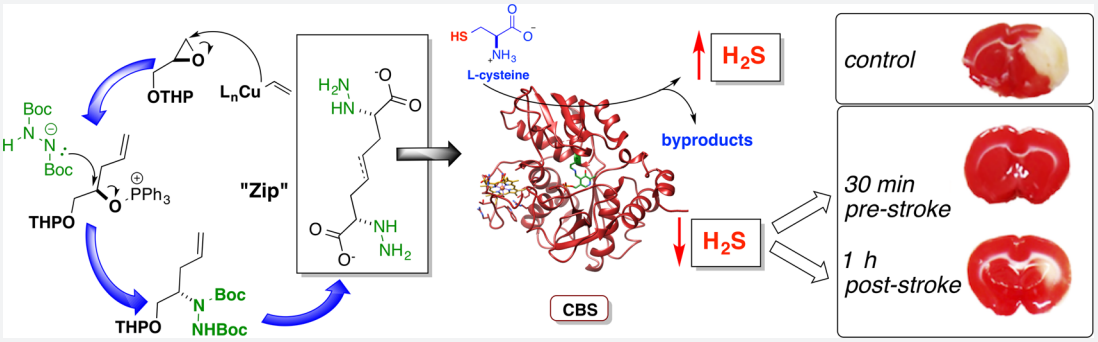

ABSTRACT: The gaseous neuromodulator H_2S is associated with neuronal cell death pursuant to cerebral ischemia. As cystathionine β-synthase (CBS) is the primary mediator of H_2S biogenesis in the brain, it has emerged as a potential target for the treatment of stroke. Herein, a "zipped" approach by alkene cross-metathesis into CBS inhibitor candidate synthesis is demonstrated. The inhibitors are modeled after the pseudo-C_2-symmetric CBS product (L,L)-cystathionine. The "zipped" concept means only half of the inhibitor needs be constructed; the two halves are then fused by olefin cross-metathesis. Inhibitor design is also mechanism-based, exploiting the favorable kinetics associated with hydrazine-imine interchange as opposed to the usual imine−imine interchange. It is demonstrated that the most potent "zipped" inhibitor **6S** reduces H_2S production in SH-SY5Y cells overexpressing CBS, thereby reducing cell death. Most importantly, CBS inhibitor **6S** dramatically reduces infarct volume (1 h post-stroke treatment; ∼70% reduction) in a rat transient middle cerebral artery occlusion model for ischemia.

INTRODUCTION

In light of evidence of H_2S production in rat, bovine, and human brain tissues,[1,2] interest has intensified in its role as the third gaseous "hormone."[3,4] In particular, H_2S appears to be an important actor in modulating cell function in the vasculature and in the cerebrum. Three enzymes[5−7] have been reported to produce H_2S endogenously, namely, (i) cystathionine β-synthase (CBS; EC 4.2.1.22), (ii) cystathionine γ-lyase (CSE; EC 4.4.1.1), and (iii) 3-mercaptopyruvate sulfurtransferase (3-MST; EC 2.8.1.2). CBS and CSE eliminate H_2S from L-cysteine, whereas 3-MST reductively releases H_2S from 3-mercaptopyruvate, itself a product of L-cysteine transamination via cysteine aminotransferase (CAT). [*In vitro*, CSE actually eliminates H_2S 3-fold more efficiently from L-homocysteine than from L-cysteine; however, physiological concentrations of the latter (100 μM) are estimated to be 10-fold higher than those of the former (10 μM), making L-cysteine the principal biological H_2S donor for CSE as well.[8]] Thioredoxin appears to be the best candidate for the *in vivo* reductant in the 3-MST reaction. Once released, H_2S may serve as (i) a signaling molecule itself or is transformed into (ii) sulfhydrated protein (e.g., through reaction with a protein disulfide), or into (iii) polysulfides or into (iv) HSNO upon reaction with NO, another prominent gaseous neuromodulator (a one electron oxidation).[9] So while the mechanism for H_2S-signaling is clearly complex, potentially divergent, and incompletely understood, important functions have been associated with H_2S-signal transduction in both the cerebrum and the vasculature.

Interestingly, all three biogenetic pathways into H_2S emanate from L-cysteine and involve a pyridoxal phosphate (PLP)-dependent enzyme. The expression of these enzymes seems to be tissue-specific. CSE has been shown to be primarily involved with H_2S production in the cardiovascular system.[10] Conversely, studies have indicated that CBS serves as the primary machinery for H_2S production in the brain, and its expression is

Received: January 19, 2016
Published: March 9, 2016

DOI: 10.1021/acscentsci.6b00019
ACS Cent. Sci. 2016, 2, 242−252

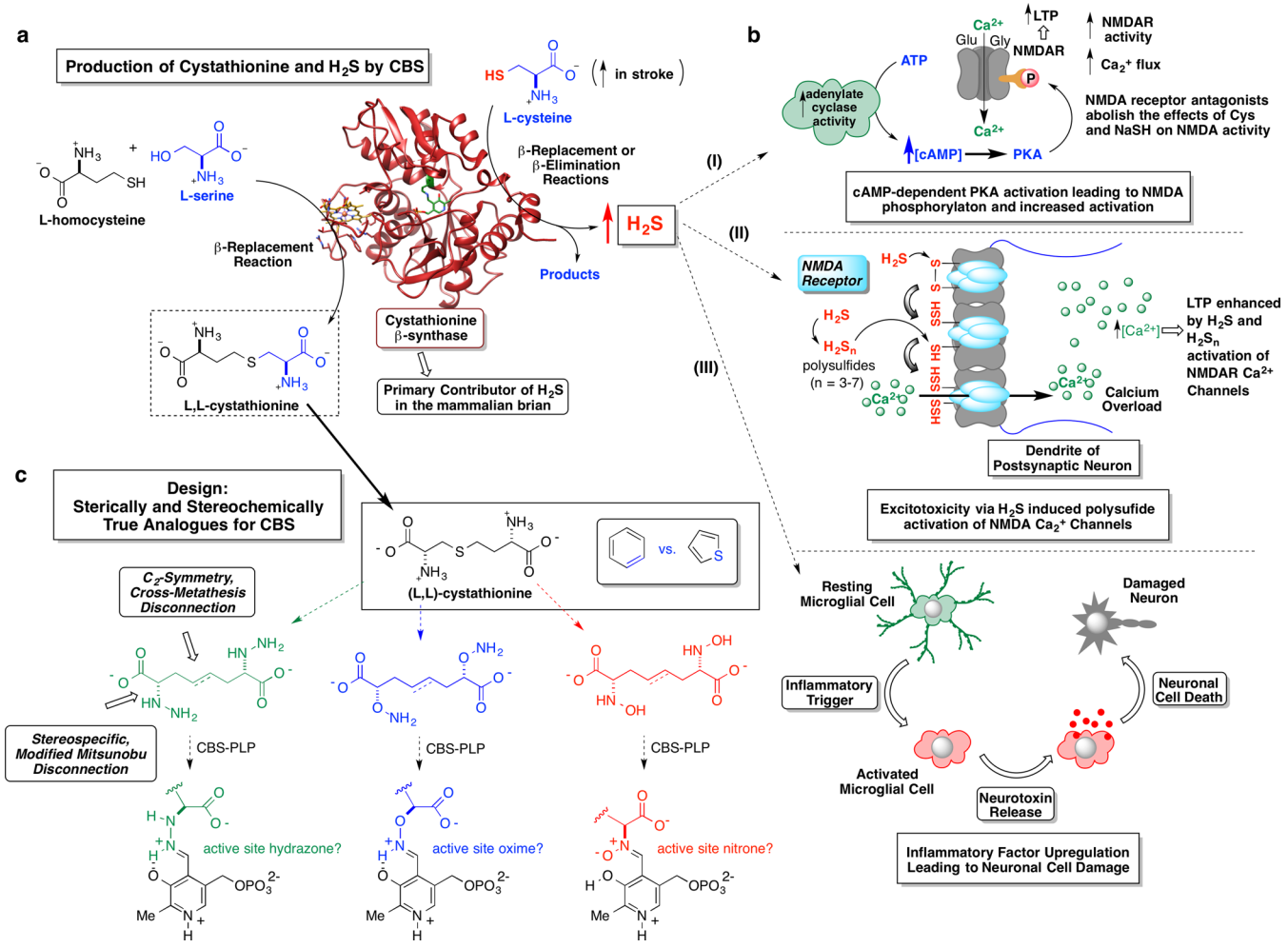

Figure 1. (a) β-Replacement reaction mediated by PLP-dependent CBS between L-serine and L-homocysteine to produce L,L-cystathionine (lower left reaction). CBS represents the primary contributor of H_2S in the mammalian brain via either β-replacement or β-elimination reactions emanating from L-cysteine (upper right reaction). (b) A few possible effects of elevated H_2S levels on neurological outcomes pursuant to stroke: (i) cAMP-dependent PKA activation leading to possible NMDA receptor phosphorylation and increased activity; (ii) H_2S enhancement of Ca^{2+} flux into the post-synaptic neuron by H_2S-release from NMDA receptor-bound polysulfides (stored sulfane sulfur); (iii) following an inflammatory trigger, elevated H_2S levels may augment signaling pathways involved in activating inflammatory cells (microglial cells) causing a discharge of mediators such as chemokines and cytokines that could further damage the neuron, exacerbating neuronal cell death. (c) Schematic illustrating the design principles of a library of CBS-targeted affinity-based inhibitors designed to incorporate recognition features of the CBS product, L,L-cystathionine. These inhibitor candidates were envisioned to engage the active-site PLP cofactor, forming tight binding hydrazone, oxime, or nitrone adducts.

highly concentrated in the astrocytes.[11,12] Understanding of H_2S in terms of its biogenesis, *in vivo* concentration, bioenergetics, and activity is still in its infancy, with the ability to measure H_2S levels *in vivo* being one of the principal challenges, particularly given that it may be "stored" in various releasable forms. A number of recent reviews[9,13−17] on H_2S provide an overview of the complexity of signaling activities ascribed to H_2S as an effector molecule. To further our understanding of the protective and deleterious effects associated with H_2S going forward, a combination of genetics and chemical biology will likely be needed. There also is great interest in developing new and more effective H_2S-sensing platforms.[18−25] At this stage, tools that allow for the modulation of CBS activity in the astrocytes [and correspondingly of CAT/3-MST activity and/or CSE activity in the vasculature] would be valuable tools to chemical biologists seeking to understand H_2S activity as a function of tissue location; concentration; cellular conditions; and source (L-cysteine, L-homocysteine, stored sulfane repository or elemental S).

H_2S Biogenesis. Illustrated in Figure 1a are the two key biological reactions mediated by CBS (coordinates for PDB 1M54 shown).[26] The reaction on the lower left represents the role of CBS in the transsulfuration pathway through which sulfur in essential dietary L-methionine is transformed into essential cellular redox equivalents in the form of glutathione. Specifically, CBS condenses L-serine with L-homocysteine in a β-replacement reaction, producing a molecule of (L,L)-cystathionine and water. This effectively moves the sulfur atom from its L-methionine source to its L-cysteine destination. (The methyl group from L-methionine is transferred elsewhere through the sequential action of three enzymes: SAM synthetase, SAM-dependent methyl-transferases, and SAH hydrolase. The resultant L-homocysteine transfers its sulfur atom to the β-carbon of L-serine through the consecutive action of two PLP-enzymes, namely, CBS, forming (L,L)-cystathionine and CSE, breaking (L,L)-cystathionine down to L-cysteine, α-

DOI: 10.1021/acscentsci.6b00019
ACS Cent. Sci. 2016, 2, 242−252

ketobutyrate, and ammonia.) The second major CBS activity, illustrated in the upper right section of Figure 1a, represents the primary H_2S-source in the mammalian brain. A suite of CBS-mediated transformations exists, through which L-cysteine is paired with a cosubstrate to produce a molecule of H_2S, either by a β-replacement or a β-elimination reaction. Elegant and comprehensive kinetic studies by Banerjee and co-workers[27] have demonstrated (i) the promiscuity of this enzyme in accepting a variety of nucleophiles in the H_2S-generating β-replacement manifold; (ii) that the by product(s) distribution associated with H_2S production is dependent upon the available nucleophiles, their physiological concentrations, and their relevant kinetic parameters (K_m, k_{cat}, and k_{cat}/K_m); (iii) that under both maximal velocity and physiological substrate concentrations, β-replacement of cysteine by homocysteine is primarily responsible for H_2S production by CBS; and (iv) at high substrate concentrations, CBS accounts for ∼95% of the total H_2S output in the brain.

H_2S Forms and Concentrations. Estimates by a variety of techniques place endogenous cerebral H_2S concentration in the range of 1−160 μM,[1,2,9] or even sub-micromolar with a new monobromobimane-based assay.[28] It might seem that such low H_2S levels would be insufficient to induce the range of physiological responses reported. However, more recently, Shibuya et al. and others[7,29] have found that H_2S may be stored in the form of polysulfides or protein persulfides formed through the process of sulfhydration. This protein-bound sulfur appears to function as an intracellular storage form of H_2S. In these studies, H_2S is released in the presence of a redox active thiol such as thioredoxin, or perhaps glutathione. Thus, actual H_2S concentrations may vary significantly as a function of cellular redox potential. Increased calcium influx to astrocytes has also been reported to actuate release of the signaling molecule D-serine, a coagonist of the *N*-methyl D-aspartate receptor (NMDAR), thereby potentiating the H_2S-signal at this receptor while signifying possible cross-talk between two PLP-dependent enzymes in the brain, CBS and serine racemase, with attendant consequences for neuronal cell damage pursuant to stroke.

Protective vs Deleterious Effects of H_2S as a Function of Concentration. The role of H_2S in the inflammatory response, another source of neuronal damage (Figure 1b, schematic iii), has been the subject of considerable debate with both pro- and anti-inflammatory roles for H_2S having been described. Research from Whiteman has shown that the effect of H_2S on inflammation is a concentration-dependent response and is dependent upon the rate of H_2S generation.[30] The pioneering work of Abe and Kimura showed that high levels of H_2S (130 μM) selectively increase NMDAR-mediated currents in hippocampal slices.[31] Later, this same group reported (Figure 1b, schematic i) that H_2S effects on the NMDAR are associated with an increase in the secondary messenger, cAMP, suggesting the activation of adenylate cyclase.[32] Elevated H_2S levels have been implicated in a wide range of abnormalities and diseases. Relevant to the collaborative work described herein, Wong et al. observed that high plasma cysteine levels correlated with poor clinical outcome of patients suffering from acute stroke.[33] In the same study, in an experimental model for stroke on rats, middle cerebral arterial occlusion (MCAO) measurements of brain infarction volumes were elevated upon exogenous introduction (IP or ICV) of cysteine prior to the occlusion, in a dose-dependent manner. A similar effect was also observed when an H_2S donor, NaSH, was administered. The hypothesis that the cysteine effect was due to its conversion to H_2S by CBS was further supported when pretreatment with aminooxyacetic acid (AOAA), a generic PLP-enzyme inhibitor, served to counteract these effects. Confirmatory evidence for high H_2S concentrations leading to enhanced cell death under ischemia was obtained in cells overexpressing CBS after knocking in of the CBS gene.[34] Moreover, brain 3-MST activity has been seen to be down-regulated following acute stroke,[35] lending additional support to the notion that CBS is the key enzyme modulating levels of cysteine-derived H_2S in the cerebral cortex and that H_2S mediates ischemic damage pursuant to stroke.

RESULTS AND DISCUSSION

Design and "Zipped Synthesis" of CBS Inhibitor Array by Cross-Metathesis. As mentioned above, all three biogenetic routes to H_2S involve PLP-enzymes, but it is CBS that serves as the principal source of H_2S biogenesis in the brain. Given the evidence implicating elevated cerebral H_2S levels in ischemic neuronal damage, CBS inhibitor development has emerged as an area of considerable interest. Owing to the dearth of such inhibitors, previous studies have relied upon generic PLP-enzyme inhibitors such as AOAA to modulate CBS activity. To address this, a central goal of this study was to develop CBS-targeted inhibitors and explore their utility as tools for chemical biology. Indeed, the Berkowitz laboratory explores problems at the interface of synthetic organic chemistry and mechanistic enzymology,[36,37] with a long-standing interest in the inhibition of PLP-dependent enzymes.[38−44] And the Wong laboratory has made a dedicated effort to develop *in vitro* and animal models for stroke, with a particular interest in H_2S-signaling.[34,45] These complementary approaches set the stage for the collaborative chemistry/neurobiology studies detailed herein.

An array of CBS-targeted inhibitors was envisioned, based upon structural, synthetic, and mechanistic considerations. (i) Structurally, the notion was to construct a series of compounds with shape and charge complementarity to (L,L)-cystathionine, the particular CBS reaction product that presents the greatest number of binding recognition elements for the enzyme and that also exhibits the tightest binding to the enzyme ($K_m \approx 83$ μM vs mM K_m values for L-serine, L-cysteine, and L-homocysteine).[46] (ii) Synthetically, the pseudo-C_2-symmetry present in the (L,L)-cystathionine structure would provide the key to a streamlined "zipped synthesis" route into the inhibitor library. (iii) Finally, mechanistically, these inhibitors were designed by careful consideration of pyridoxaldimine chemistry in PLP-enzyme active sites. Namely, the inhibitor candidates were designed to be outfitted with vicinal heteroatomic functional groups (-$NHNH_2$, -ONH_2, -NHOH) in place of the usual α-amino groups. This is because such derivatives have the potential to display especially favorable binding kinetics with respect to cofactor-adduction. This is borne out by a careful survey of the literature, as is laid out in detail in Figure S10 of the Supporting Information. Whereas for α-hydrazino acids, imine-hydrazone interchange (i.e., transaldimination) is 1−2 orders of magnitude slower than the corresponding imine−imine interchange for native α-amino acid substrates in the forward direction (i.e., k_{on}), the reverse reaction is some 4−6 orders of magnitude slower (i.e., k_{off}) for the former ($t(1/2)_{off} \approx 0.02-1$ s) vs the latter ($t(1/2)_{off} \approx 2.5$ h). In simple terms, the price that one pays in terms of attenuated k_{on} kinetics is more than compensated for by greatly diminished k_{off} rates for the α-hydrazino-acids vs α-amino-acids resulting in an

DOI: 10.1021/acscentsci.6b00019
ACS Cent. Sci. 2016, 2, 242−252

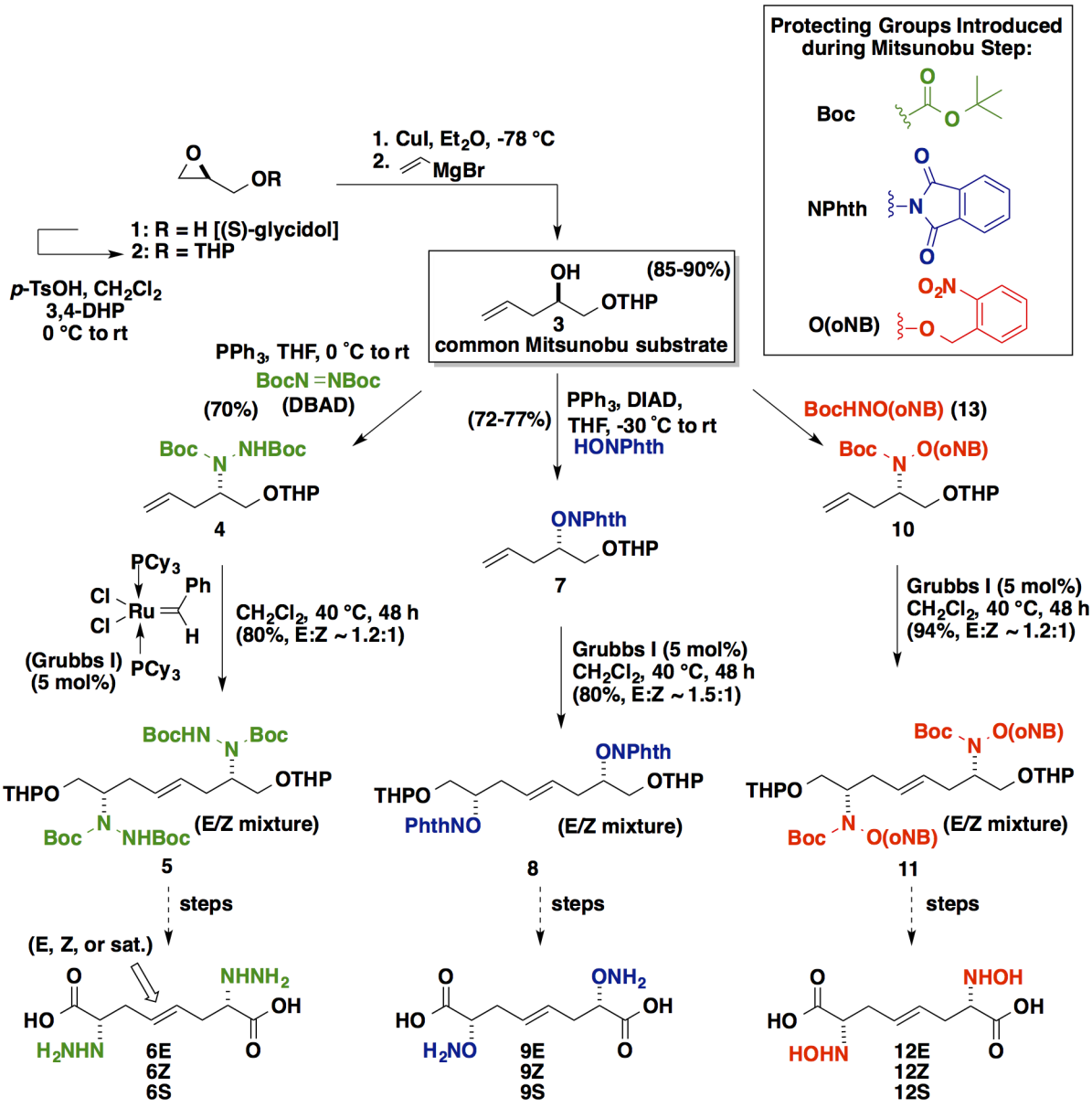

Figure 2. Detailed routes for the "zipped synthesis" of the array of CBS inhibitor candidates.

anticipated ~10^3-fold advantage in effective equilibrium constant for covalent cofactor adduction for such compounds.

Following this analysis, we chose to design our library as is illustrated in Figure 1c, retrosynthetically replacing the central thioether linkage with an "isosteric" C=C linkage. (Consider here the difficulty of separating thiophene impurities from benzene. In this case, after replacing the central S with at C=C element, a single methylene is removed so as convert a pseudosymmetric inhibitor target into a perfectly symmetrical one). This introduces actual C_2-symmetry into the inhibitor design, and, most importantly, enables these inhibitors to be "zipped" together by Grubbs cross-metathesis chemistry[47] from a single "half-inhibitor" precursor, greatly streamlining the chemistry. The broad functional group compatibility[48] of the metathesis chemistry makes it especially appropriate for this application in chemical biology. Highlighted in Figure 2 are the key synthetic transformations leading to the focused library of CBS inhibitor candidates targeted herein. Starting from (*S*)-glycidol, *O*-THP-protection, and vinyl cuprate-mediated epoxide ring-opening efficiently yield the important D-*α*-hydroxy-4-pentenol-derived chiral synthon **3**. Compound **3** proved to be a key common intermediate for a series of modified Mitsunobu reactions (~70% yield for each series) in which the C*α*-hydroxyl group is stereospecifically substituted with an *α*-effect nucleophile, with inversion of configuration, giving (i) the bis-Boc-protected hydrazine **4**, (ii) the *N*-phthalimide-protected aminooxy compound **7**, or (iii) the *N*-Boc-*O*-*o*-nitrobenzyl-protected hydroxylamine **10**. The zipped approach of streamlining the construction of such inhibitors by exploiting C_2-symmetry proved to be quite effective, allowing for swift assembly of the carbon backbone via convergent alkene cross-metathesis. The Grubbs first generation catalyst serves to zip together the two halves of the targeted inhibitors quite cleanly ("spot to spot" reactions, albeit with two geometric isomers being formed; ~80% yields). Following these convergent cross-metathesis transformations, tailoring chemistry was performed in order to separate the geometric isomers and set the desired oxidation state. These operations

DOI: 10.1021/acscentsci.6b00019
ACS Cent. Sci. 2016, 2, 242−252

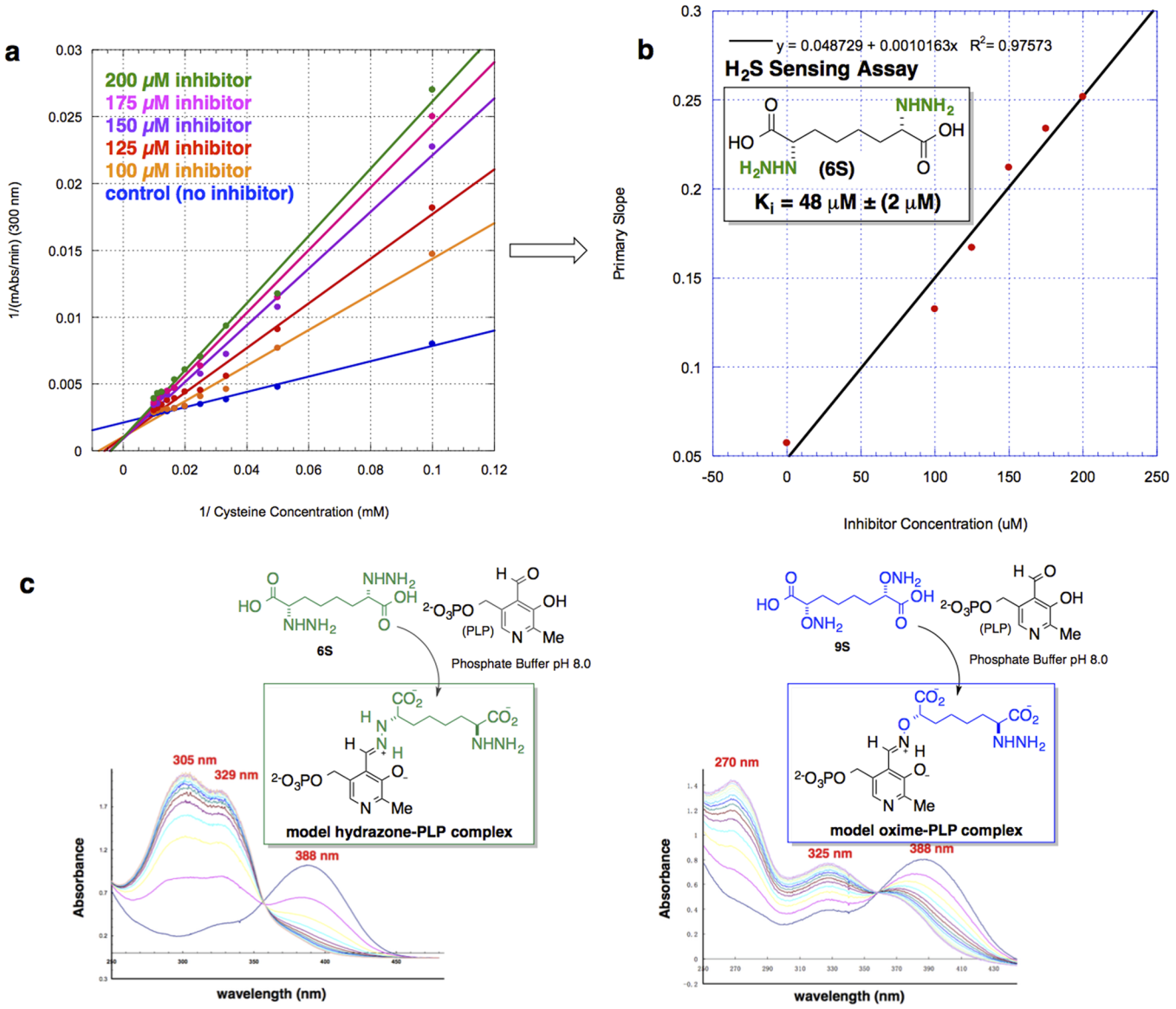

Figure 3. Results from kinetic analysis of inhibitor candidates with the hCBS truncated dimer. (a) Lineweaver−Burk plot for hCBS inhibition with **6S**, detecting H_2S production in the presence $Pb(OAc)_2$. (b) Secondary-plot of bis-α-hydrazino acid (**6S**) inhibition of H_2S production by hCBS yielding a K_i value of 48 ± 2 μM. (c) UV/vis spectroscopic profile of model PLP-inhibitor adducts formed nonenzymatically. Conditions: 0.26 mM hydrazino acid **6S**, 0.2 mM PLP, 50 mM KPO_4 (pH 8.0), scans every 10 min, isosbestic point = 355 nm, $t_{1/2}$ = 7 min (left spectrum); conditions: 0.33 mM aminooxy acid **9S**, 0.2 mM PLP, 50 mM KPO_4 (pH 8.0), scans recorded every 10 min, isosbestic point = 360 nm, $t_{1/2}$ = 15 min (right spectrum).

include (i) *O*-THP-deprotection, (ii) Jones oxidation, and finally (iii) a convenient global deprotection strategy to unveil a 3 × 3 array of CBS inhibitor candidates.

Enzyme Kinetics: CBS Inhibition Studies. CBS inhibition assays were performed on the heterologously expressed human enzyme, hCBSΔC143 construct. This truncated form of the enzyme lacking the C-terminal regulatory domain is known to form a highly active dimeric enzyme that has been characterized structurally.[49] A comprehensive assessment of inhibitor candidate fitness was conducted utilizing three distinct assays for hCBS activity: (i) a modified continuous assay, exploiting microscopic reversibility, allowed for measurement of the cystathionine-lyase activity of hCBS, followed by trapping of the L-homocysteine produced with 5,5′-dithiobis(2-nitrobenzoic acid) (DTNB, Ellman's reagent) and spectroscopically quantifying the *m*-carboxy-*p*-nitrothiophenolate anion (λ_{max} = 412 nm; $\Delta\varepsilon_{412}$ = 13 600 M^{-1} cm^{-1}) thereby released; (ii) a radioactive label-based assay reporting on the forward trans-sulfuration reaction catalyzed by hCBS using ^{14}C-labeled L-serine in the presence of L-homocysteine to measure ^{14}C-labeled (L,L)-cystathionine product. And, most importantly, (iii) a modified H_2S-sensing assay to measure hCBS-catalyzed production of H_2S from L-cysteine. Capture of the H_2S produced by $Pb(OAc)_2$ leads to the formation of PbS and a concomitant increase in Abs_{300} (Figure 3a,b).

Both the (L,L)-cystathionine lyase-activity and radioactive assay identified the fully saturated α-(L,L)-bis-hydrazino acid **6S** to be the most potent CBS inhibitor candidate (see Supporting Information). Furthermore, It should be noted that assays involving the hydroxylamino acid compounds **12E**, **12Z**, and **12S** (designed as "nitrone-formers") were not compatible with the continuous assay. When tested in the radioactive assay, both

DOI: 10.1021/acscentsci.6b00019
ACS Cent. Sci. 2016, 2, 242−252

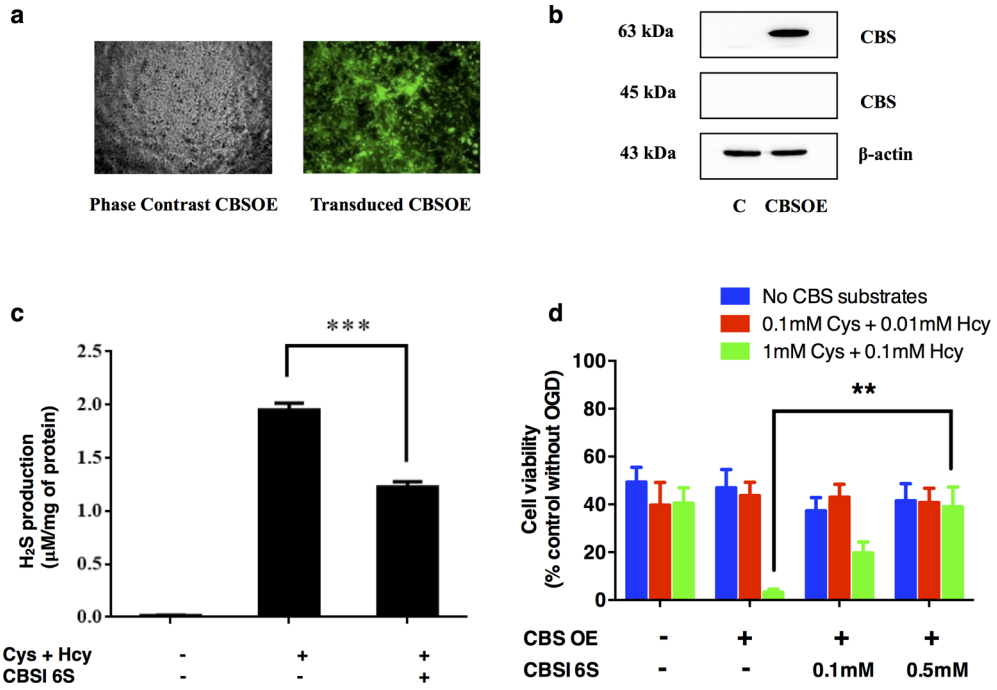

Figure 4. Reversal of enhanced cell death in CBS-overexpressing (CBSOE) SH-SY5Y cells exposed to high CBS substrates by CBS inhibitor **6S**. (a) Fluorescence (right) and phase contrast (left) micrographs of lentiviral vector transduced SH-SY5Y CBSOE cells. Fluorescence indicates CBS-EGFP (reporter gene) expression. (b) Western blot results confirming that CBS was markedly expressed compared to nontransduced control (C) cells. Only the full length CBS (63 kDa) was detected but not the truncated CBS (45 kDa). (c) Inhibition by CBS inhibitor (CBSI) **6S** of H_2S production in SH-SY5Y CBSOE cell homogenates in the presence of L-cysteine (1 mM) and L-homocysteine (0.1 mM). Data are presented as mean ± SEM, n = 3. ANOVA: F (2, 6) = 421.247, $p < 0.05$; ***$p < 0.001$ against no inhibitor control by Bonferroni. (d) CBS inhibition by **6S** reversed the enhanced cell death in CBSOE cells subjected to OGD (24 h) in the presence of high substrates. Cell viability is expressed as fraction to control without OGD (not shown). ANOVA for high substrate conditions: F (3, 11) = 10.248, $p < 0.05$; **$p < 0.01$ against without **6S** by Bonferroni. Data are mean ± SEM, n = 3–4.

the aminooxy (-ONH_2 series) and hydrazino acid (-$NHNH_2$ series) inhibitor classes significantly outperformed the hydroxylamino acid class (-NHOH series). This is consistent with the spectroscopic studies involving incubation with PLP directly (see below and Figure 3c), the results of which point to the greater predilection of PLP to engage in hydrazone (-$NHNH_2$ series) and oxime (-ONH_2 series) linkages, in comparison with nitrone linkages (-NHOH series). Given the promise associated with the hydrazone-forming strategy in particular here, further kinetic analysis was performed on the most promising inhibitor candidate, **6S**, this time monitoring its effect on CBS-mediated H_2S formation directly. Using the aforementioned Pb-based spectrophotometric H_2S sensing assay, **6S** was found to display a kinetic pattern consistent with clean competitive inhibition of the CBS with respect to L-cysteine, yielding K_i = 48 ± 2 μM.

As noted, to test the inhibitor design strategy, a series of model experiments was conducted by incubation of specific inhibitor candidates of each functional group class with PLP in solution. PLP-adduct formation with the saturated inhibitor candidates **6S**, **9S**, and **12S** was monitored by UV/vis spectroscopy (Figure 3c). These model experiments were deemed particularly important because hCBS contains a critical heme domain that absorbs broadly in the UV/vis from 325 to 500 nm,[49] thereby blocking the spectral region in which one typically observes the active site internal PLP-aldimine (λ_{max} ≈ 420 nm) and related PLP-adducts. Displayed in Figure 3c are the spectroscopic profiles of compound **6S** and **9S**, respectively, upon incubation with PLP. For each model experiment, the spectrum indicates that at t = 0 no complex has formed. The absorption peak at λ_{max} = 388 nm is attributed to free PLP; over time, additional peaks appear and the peak at 388 nm diminishes as covalent cofactor adduct formation proceeds. The projected hydrazone-forming compound **6S**, for example, when incubated with PLP, gives rise to absorbance peaks at 305 and 329 nm. A different spectroscopic signature for the putative oxime-former **9S** appears with absorbances at 270 and 325 nm. It should be noted that the saturated *N*-hydroxy amino acid compound **12S** was also tested in the same manner. However, the data do not provide evidence for the formation of a stable nitrone adduct with the cofactor under these conditions. The apparent PLP-hydrazone, on the other hand, is reminiscent of the carbidopa hydrazone that forms in the active site of peripheral DOPA decarboxylase (combination therapy for Parkinson's disease).[50,51] Indeed, in spectroscopic studies conducted for carbidopa[52] (100 μM) and PLP (10 μM) alone, hydrazone formation was characterized by two absorption bands at λ_{max} = 305 and 335 nm ($t_{1/2}$ = 1.19 min) and a shoulder around 380 nm. Thus, the preponderance of evidence suggests that **6S** and **9S** are able to engage the PLP cofactor in stable hydrazone and oxime adduct linkages, respectively, but it remains an open question as to whether **12S** can engage the cofactor in a stable nitrone linkage, at least in aqueous solution. Given these encouraging results, compound **6S** was advanced into the chemical biology stage of the investigation, including examination of performance in both *in vitro* cell-based assay and *in vivo* assay using a rat middle cerebral artery occlusion model for stroke.

Neuronal Cell Culture: Oxygen/Glucose Deprivation (OGD) Model Studies. Pleasingly, experiments designed to test the ability of **6S** to attenuate the H_2S-synthesizing activity

DOI: 10.1021/acscentsci.6b00019
ACS Cent. Sci. 2016, 2, 242–252

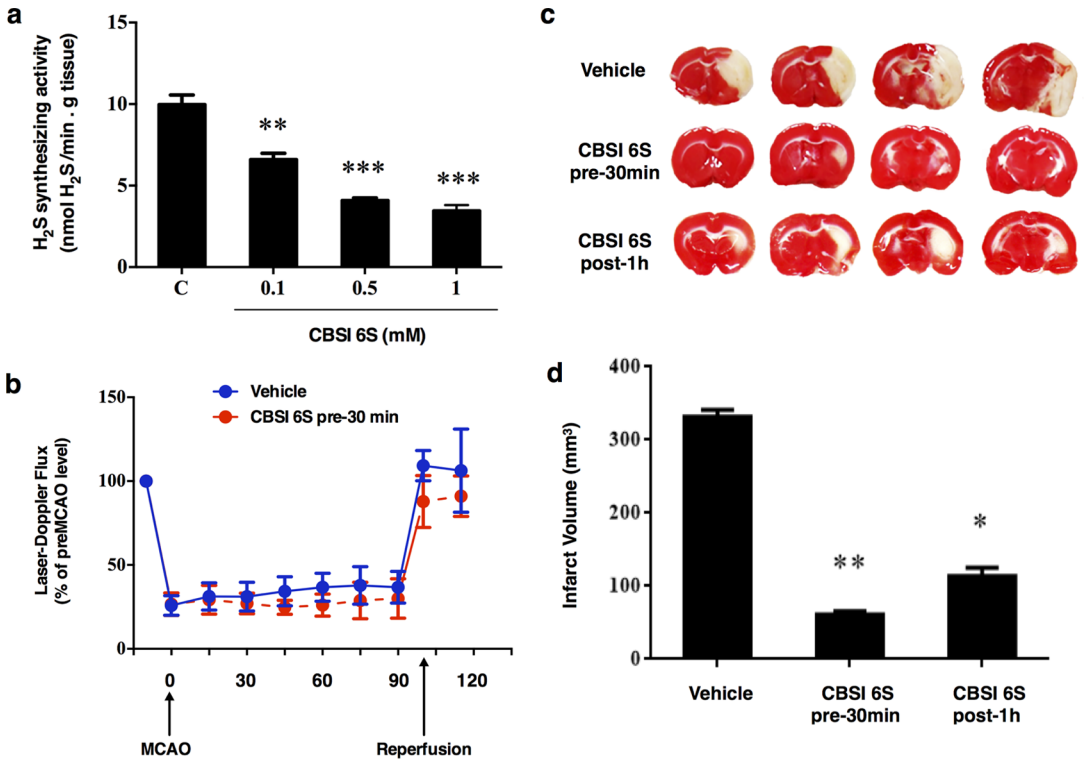

Figure 5. Neuroprotection by CBS inhibitor **6S** against ischemic injury induced by transient middle cerebral artery occlusion (tMCAO). (a) Inhibition of H_2S synthesizing activity in brain homogenate at varying concentrations of CBSI 6S. Data are presented as mean ± SEM, $n = 3–7$; $^{**}p < 0.01$, $^{***}p < 0.001$ against no inhibitor control (C) by Bonferroni. (b) The right MCA was occluded by the insertion of a suture through the carotid artery for 100 min. The blood flow in the affected area was monitored by a Laser-Doppler device showing a reduction of about 70−75% and returned to pre-MCAO levels upon reperfusion, $n = 7–10$. (c) Infarct volumes at 24 h after tMCAO. Top panel shows representative TTC-stained forebrain sections of a vehicle-treated, a CBSI **6S**-pretreated and a CBSI **6S**-post-treated rat. CBSI **6S** or vehicle was administered by intracerebroventricular (icv) injection 30 min before tMCAO (CBSI pre-30 min) or 1 h after middle cerebral artery occlusion (CBSI post 1 h). (d) Bottom panel shows the calculated infarct volumes of the three groups, $n = 5–10$, ANOVA: $F(2, 19) = 7.89$, $^{*}p < 0.05$, $^{**}p < 0.01$ against vehicle control group by Bonferroni.

in brain whole cell lysates were consistent with the *in vitro* kinetic assays previously described ($K_i \approx 50$ μM for H_2S production). Moreover, in neuroblastoma model studies simulating ischemic conditions through oxygen and glucose deprivation (OGD) (Figure 4), SH-SY5Y overexpressing CBS (CBSOE cells) were treated with concentrations of L-cysteine and L-homocysteine that represent estimated physiological substrate concentrations (red),[53] on the one hand, and high concentrations (green), on the other. These experiments were conducted in the absence or presence of CBS inhibitor **6S** (100 and 500 μM). As shown in Figure 4, the cell viability of CBSOE cells was reduced to ∼50% when subjected to OGD for 24 h. When physiological substrate concentrations were used, there was no significant change in cell viability as compared to the no substrate control. However, when substrate concentrations were increased 10-fold to mimic stroke conditions, a significant loss in cell viability to <10% was observed, presumably due to the high levels of H_2S production through the action of CBS.[34] As expected, cell viability was largely restored by addition of inhibitor **6S**. Indeed, the SH-SY5Y CBS overexpressing cells responded in a dose-dependent manner (see Figure S16 in the Supporting Information for details) to rescue with **6S**, with nearly full restoration to control levels being observed at 500 μM of inhibitor. These results are consistent with reports that the effects of H_2S on neuronal damage[33,54] and macrophages[55] are dependent on the H_2S concentration at the time of insult.

Rat Stroke Model: Transient Middle Cerebral Artery Occlusion (tMCAO). Next, an *in vivo* tMCAO rat model study was undertaken to ascertain whether the observed inhibition of CBS *in vitro*, and inhibition of H_2S biogenesis in SH-SY5Y CBS overexpressing cells lysate by **6S** would translate into attenuation of infarction volume in a rat stroke model. In the event, the middle cerebral artery was transiently blocked for 100 min to induce tissue infarction in the following 24 h window. Illustrated in Figure 5, infarct volumes were determined in brain slices stained with TTC (2,3,5-triphenyl-2H-tetrazolium chloride). In this assay, tissues undergoing active respiration exhibit significant succinate dehydrogenase activity and this manifests itself in reduction of the TTC indicator, producing triphenylformazan (TPF) a red-colored dye. By contrast, those regions suffering from necrosis exhibit a markedly lower local redox potential, and fail to reduce the tetrazolium salt to the corresponding formazan dye, resulting in unstained regions indicative of infarction. The volume of unstained tissue relative to the hemispherical volume was then experimentally quantified and used as a measure of infarction volume. As can be seen in Figure 6c, this lead compound **6S** (1.6 μmol/kg, intracerebroventricular injection) protected against infarction, with an 83% or 66% reduction in infarction volume being seen, relative to control when the inhibitor was injected 30 min prior to or 60 min after the start of tMCAO, respectively. These results clearly demonstrate a pharmacological effect of the inhibitor in an *in vivo* setting. In addition, **6S**

DOI: 10.1021/acscentsci.6b00019
ACS Cent. Sci. 2016, 2, 242−252

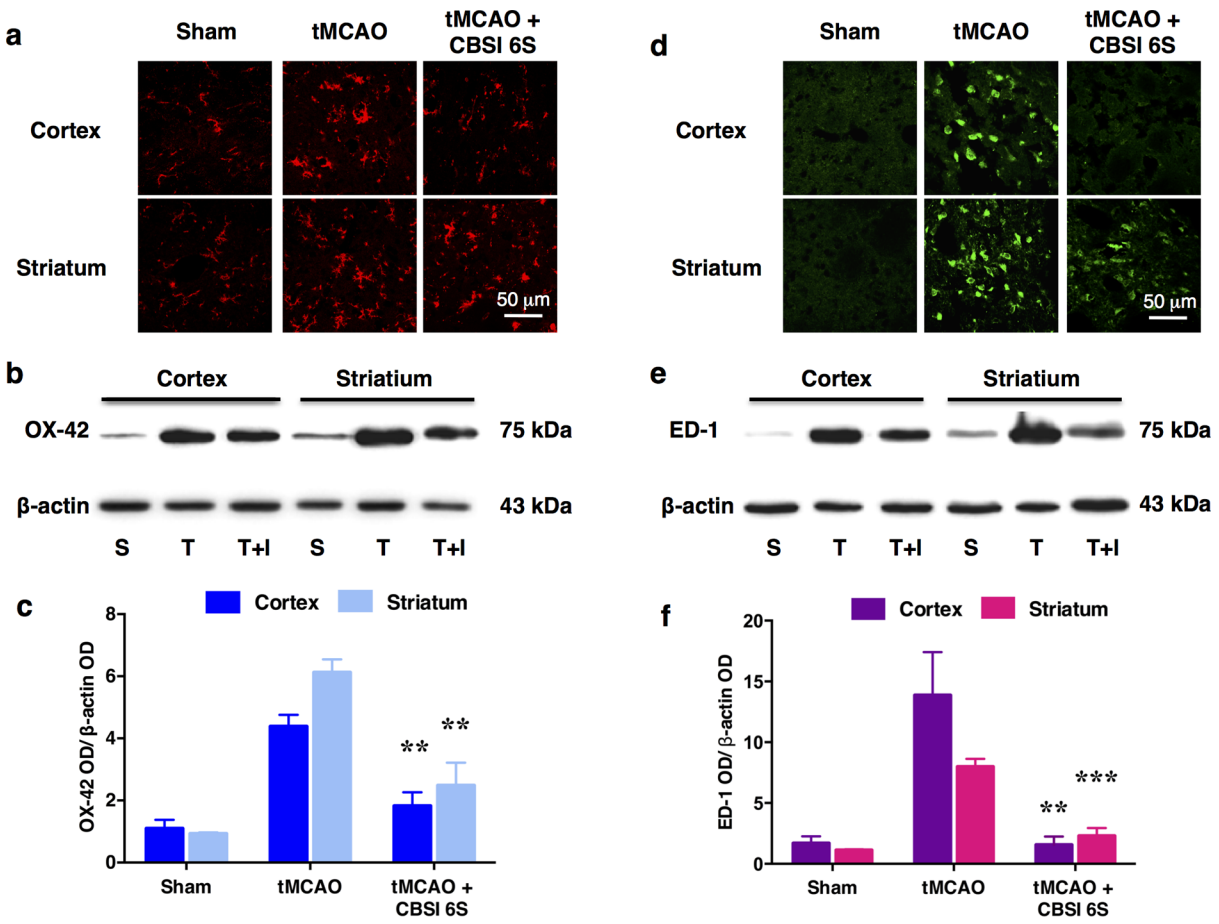

Figure 6. Reduction of microglial number and activation of the MCAO-affected cortex (Co) and striatum (St) by CBS inhibitor **6S**. (a) OX-42-immunopositive microglial cells observed in the Sham-operated (S) group are resting microglia based on their ramified star-like morphology. Marked increase in the number of microglia was observed in the tMCAO (T) group. Many of these cells are activated as they appeared to be large with thick processes. In the CBSI **6S**-treated tMCAO (T + I) group, the number of activated microglia was reduced although still increased when compared to the Sham group. (b) Representative Western blot results. (c) Quantified Western blot results, $n = 3-4$. ANOVA: $F(2, 8) = 19.399$ for cortical OX-42, $F(2, 8) = 25.288$ for striatal OX-42, $^{**}p < 0.01$ against respective tMCAO (T) group by Bonferroni. Western blot results support the observations in A. (d–f) are similar to (a–c) except that they are for ED-1 which is a marker of macrophages including phagocytic microglia, which are comparatively absent in the sham group. (f) ANOVA: $F(2, 8) = 15.408$ for cortical ED-1 and $F(2, 7) = 59.718$ for striatal ED-1, $^{**}p < 0.01$, $^{***}p < 0.001$ against respective tMCAO (T) group by Bonferroni.

appeared to have no effect on cerebral blood flow as observed in the first 30 min after administration but before the onset of tMCAO in the pretreatment group (Figure 5b). The fact that this inhibitor remained effective when given as a post-stroke treatment following the onset of occlusion is encouraging as this is the norm in the treatment of acute stroke.

Modulating the Microglial Response in the Presence of the CBS Inhibitor. In light of these encouraging results, experiments were also conducted to examine whether the dramatic reduction in infarct volume observed upon ICV treatment with **6S** might correlate with a reduction in microglial activation. Microglia account for 10–15% of all brain cells. In the normal brain, microglia exist as ramified star-like cells known as resting microglia. In disease or injury, microglia are first transformed into activated microglia with thicker processes and larger cell bodies, and then into large amoeboid shape phagocytic microglia. They function as scavengers through phagocytosis of dead/apoptotic cells, cellular debris, and foreign materials such as viruses and bacteria. They can also release cytotoxic free radicals and activate pro-inflammatory cytokines and chemokines. Figure 6a shows OX-42 immunopositive microglia in the cortex and striatum. Resident microglia mostly in the resting state can be seen in the sham-operated group. The tMCAO group shows microglial activation as evidenced by the increase in number and change in morphology. However, treatment with CBS inhibitor **6S** markedly attenuates the microglial activation. Furthermore, staining for ED-1, a marker for macrophages including phagocytic microglia, shows many such cells in the tMCAO group. This marker, too, was correspondingly reduced in the CBS inhibitor-treated group. In contrast, macrophages are not detected in the sham-operated group (Figure 6d). These observations are supported by the Western blot data (Figure 6b,c and e, f). Overall, treatment with **6S** leads to a significant decrease in microglial activation as a result of reduced tissue damage induced by tMCAO. These results provide support for the idea that targeted blockade of H_2S-production in ischemic tissues may dampen the inflammatory response, in addition to attenuating infarction.

CONCLUSIONS

The studies described herein articulate design elements for the inhibition of hCBS that are likely generalizable to other enzyme targets, particularly those dependent upon PLP. These design

DOI: 10.1021/acscentsci.6b00019
ACS Cent. Sci. 2016, 2, 242–252

principles include (i) choosing that enzymatic product, (L,L)-cystathionine here, that presents the largest binding surface as a platform for inhibitor design, even if that product is not produced in the reaction being targeted for tissue-localized inhibition (H_2S production here). Next, (ii) the pseudo-C_2-symmetry in the cognate substrate may be exploited to greatly simplify inhibitor candidate construction, by allowing for the stereocontrolled synthesis of one-half of the inhibitor structure, in this case, followed by a melding of the two halves by a quite efficient Ru-mediated alkene cross-metathesis transformation mediated by the Grubbs first generation catalyst. Finally, (iii) these studies support the use of an X-Y affinity reagent functionality in place of the α-amino group to develop PLP enzyme inhibitor candidates, but, at the same time, point to the advantage of surveying a range of such X-Y functionalities as significant structure/activity relationship (SAR) may be seen.

Indeed, key results here include the observation that CBS inhibitors mimicking the (L,L)-cystathionine structure but bearing α-hydrazino functionality in place of the α-amino groups are most effective in blocking hCBS activity, presumably via active site PLP-hydrazone formation, consistent with model studies. The most effective inhibitor, **6S**, displays a K_i lower than the best substrate K_m yet reported (for (L,L)-cystathionine itself) and, to our knowledge, the lowest K_i reported to date for a competitive inhibitor of the enzyme. Compound **6S** also exhibits functional irreversible inhibition (exhaustive dialysis studies show essentially no recovery of CBS activity against two different buffer systems; see Figure S13 and the surrounding experimental details in the Supporting Information) and consistently curtails CBS activity across three different assay platforms − (i) cystathionine lyase and (ii) formation activities (bidirectional transsulfuration) and (iii) H_2S evolution. Given the ability of this model inhibitor to effectively block CBS-based evolution of H_2S from L-cysteine in purified enzyme assays, compound **6S** was employed as a chemical biological tool to manipulate H_2S levels in both cell culture model systems and in an animal stroke model.

These studies show promise for the ICV delivery of hCBS inhibitors to neuronal tissue on several fronts. First, the efficacy of the C_2-symmetric hydrazone former, **6S**, in competitively inhibiting H_2S formation in the cuvette is mirrored when assaying its effect on H_2S evolution in neuronal cell tissue culture. Second, in SH-SY5Y cerebral neuronal cell model studies employing OGD and high L-cysteine/L-homocysteine concentrations to mimic stroke-like conditions, **6S** is seen to improve cell viability. Third, this protective effect of **6S** in cell culture translates into a protective effect against cerebral infarction in a rat tMCAO model, over a 100 min occlusion window. Infarction volume is reduced by over 80% upon ICV pretreatment with **6S** (at 1.6 μmol/kg) 30 min prestroke and by nearly 70% when treatment is 1 h post-stroke. These observations point to the utility of simple chemical biological tools in projecting out toward an eventual therapeutic window for an actual treatment. Finally, in separate experiments, treatment with **6S** is also seen to dampen the inflammatory response associated with ischemia as measured by the up-regulation of the macrophage and phagocyte-specific markers, OX42 and ED1, respectively, in the tMCAO rat model and their subsequent knockdown upon **6S** treatment, in both the cerebral cortex and striatum.

The principles articulated here with respect to CBS inhibitor (i) structure (exploiting the pseudo-C_2-symmetry inherent in L,L-cystathionine), (ii) synthesis (demonstration of an efficient "zipped synthesis" based upon versatile cross-metathesis chemistry) and (iii) mechanism (exploiting the slow k_{off} rate associated with PLP-enzyme imine-hydrazone interchange—$t(1/2)_{off} \approx 2.5$ h) will likely inform future efforts toward enzyme inhibitor design, in general, and targeted efforts toward blocking enzyme activity dependent upon pyridoxal phosphate, in particular. Compound **6S**, the first generation chemical biological tool introduced here, though not highly potent, represents a great improvement upon aminooxyacetic acid (AOAA), the relatively nonspecific PLP enzyme inhibitor that has been used in the closest previous studies. As a first pass measure of specificity, GABA AT was used as a comparison enzyme, as this is one of the best studied PLP-enzymes and one of the most important PLP enzymes in the brain (controls brain GABA levels). Whereas **6S** is a 12-fold better inhibitor of CBS ($K_i \approx 48$ μM) than of GABA AT (IC(50) $\approx$ 572 μM), AOAA is a 33-fold better inhibitor of GABA AT (IC(50) $\approx$ 360 nM) than of CBS (IC(50) $\approx$ 12 μM)[54] (see Figure S17 in the Supporting Information for details of the specificity assays). Taken together these data show that **6S** has a 400-fold specificity advantage over AOAA for CBS inhibition as opposed to GABA AT inhibition.

Of course, moving forward, it will be desirable to fine-tune the inhibitor designs identified herein so as to expand and refine the arsenal of chemical biological tools available for the study of this important hCBS enzyme. Lead compound **6S** provides a useful starting point for such studies and sets the stage for the development of second generation hCBS inhibitors wherein issues of bioavailabilty, transport, metabolism, and conformity to Lipinski's rules of five[56−58] may be addressed. As was discussed at the outset, there is a major need today to better define the temporal and spatial distribution of H_2S biogenesis and to better understand both the biological roles of H_2S and the molecular mechanisms by which these are achieved. This study demonstrates the important role that small molecule enzyme modulators are likely to play in addressing these important questions in neuronal biology.

■ ASSOCIATED CONTENT

Supporting Information

The Supporting Information is available free of charge on the ACS Publications website at DOI: 10.1021/acscentsci.6b00019.

Details of the synthesis, complete characterization of new compounds, and procedures for all enzyme kinetics, cell culture, and animal model studies (PDF)

■ AUTHOR INFORMATION

Corresponding Authors

*(D.B.D.) E-mail: dberkowitz1@unl.edu.

*(P.T.-H.W.) E-mail: peter_wong@nuhs.edu.sg.

Author Contributions

The project was designed by P.T.-H.W. and D.B.B. with assistance from all of the authors. C.D.M., M.L.B., W.S., and W.J.C. performed the chemical synthesis. C.D.M., M.L.B., W.S., and L.S. performed the *in vitro* enzyme assays. S.J.C., C.C., and S.Q.K. performed the cellular and rat stroke model studies. All authors analyzed the data and C.D.M., S.J.C., M.L.B., P.T.-H.W., and D.B.B. wrote the manuscript.

Notes

The authors declare no competing financial interest.

DOI: 10.1021/acscentsci.6b00019
ACS Cent. Sci. 2016, 2, 242−252

■ ACKNOWLEDGMENTS

This research was facilitated by the Individual Research and Development (IR/D) Program associated with D.B.B.'s appointment at the National Science Foundation. D.B.B. thanks the American Heart Association, the NIH (SIG-1-510-RR-06307), and the NSF (1500076) for funding in support this research and the NIH (RR016544) for facilities renovation. P.T.-H.W. acknowledges support from the NRF (CRP3-2008-01) and the BMRC (08/1/21/19/559). L.M.S. thanks the NSF REU program (1460829) for support of undergraduate research on this project.

■ REFERENCES

(1) Goodwin, L. R.; Francom, D.; Dieken, F. P.; Taylor, J. D.; Warenycia, M. W.; Reiffenstein, R.; Dowling, G. Determination of sulfide in brain tissue by gas dialysis/ion chromatography: Postmortem studies and two case reports. *J. Anal. Toxicol.* **1989**, *13*, 105−109.

(2) Warenycia, M. W.; Goodwin, L. R.; Benishin, C. G.; Reiffenstein, R.; Francom, D. M.; Taylor, J. D.; Dieken, F. P. Acute hydrogen sulfide poisoning: Demonstration of selective uptake of sulfide by the brainstem by measurement of brain sulfide levels. *Biochem. Pharmacol.* **1989**, *38*, 973−981.

(3) Kajimura, M.; Fukuda, R.; Bateman, R. M.; Yamamoto, T.; Suematsu, M. Interactions of multiple gas-transducing systems: Hallmarks and uncertainties of CO, NO, and H_2S gas biology. *Antioxid. Redox Signaling* **2010**, *13*, 157−192.

(4) Leffler, C. W.; Parfenova, H.; Jaggar, J. H.; Wang, R. Carbon monoxide and hydrogen sulfide: Gaseous messengers in cerebrovascular circulation. *J. Appl. Physiol.* **2005**, *100*, 1065−1076.

(5) Erickson, P.; Maxwell, I.; Su, L.; Baumann, M.; Glode, L. Sequence of cDNA for rat cystathionine gamma-lyase and comparison of deduced amino acid sequence with related *Escherichia coli* enzymes. *Biochem. J.* **1990**, *269*, 335−340.

(6) Swaroop, M.; Bradley, K.; Ohura, T.; Tahara, T.; Roper, M. D.; Rosenberg, L.; Kraus, J. Rat cystathionine beta-synthase. Gene organization and alternative splicing. *J. Biol. Chem.* **1992**, *267*, 11455−11461.

(7) Shibuya, N.; Tanaka, M.; Yoshida, M.; Ogasawara, Y.; Togawa, T.; Ishii, K.; Kimura, H. 3-mercaptopyruvate sulfurtransferase produces hydrogen sulfide and bound sulfane sulfur in the brain. *Antioxid. Redox Signaling* **2009**, *11*, 703−714.

(8) Chiku, T.; Padovani, D.; Zhu, W.; Singh, S.; Vitvitsky, V.; Banerjee, R. H_2S biogenesis by human cystathionine gamma-lyase leads to the novel sulfur metabolites lanthionine and homolanthionine and is responsive to the grade of hyperhomocysteinemia. *J. Biol. Chem.* **2009**, *284*, 11601−11612.

(9) Kimura, H. Signaling molecules: Hydrogen sulfide and polysulfide. *Antioxid. Redox Signaling* **2015**, *22*, 362−376.

(10) Yang, G.; Wu, L.; Jiang, B.; Yang, W.; Qi, J.; Cao, K.; Meng, Q.; Mustafa, A. K.; Mu, W.; Zhang, S.; et al. H_2S as a physiologic vasorelaxant: Hypertension in mice with deletion of cystathionine γ-lyase. *Science* **2008**, *322*, 587−590.

(11) Enokido, Y.; Suzuki, E.; Iwasawa, K.; Namekata, K.; Okazawa, H.; Kimura, H. Cystathionine β-synthase, a key enzyme for homocysteine metabolism, is preferentially expressed in the radial glia/astrocyte lineage of developing mouse CNS. *FASEB J.* **2005**, *19*, 1854−1856.

(12) Lee, M.; Schwab, C.; Yu, S.; McGeer, E.; McGeer, P. L. Astrocytes produce the antiinflammatory and neuroprotective agent hydrogen sulfide. *Neurobiol. Aging* **2009**, *30*, 1523−1534.

(13) Qu, K.; Lee, S. W.; Bian, J. S.; Low, C. M.; Wong, P. T. Hydrogen sulfide: Neurochemistry and neurobiology. *Neurochem. Int.* **2008**, *52*, 155−165.

(14) Kimura, H. The physiological role of hydrogen sulfide and beyond. *Nitric Oxide* **2014**, *41*, 4−10.

(15) Majid, A. Neuroprotection in stroke: Past, present, and future. *ISRN Neurology* **2014**, *2014*, 1−17.

(16) Módis, K.; Bos, E. M.; Calzia, E.; van Goor, H.; Coletta, C.; Papapetropoulos, A.; Hellmich, M. R.; Radermacher, P.; Bouillaud, F.; Szabo, C. Regulation of mitochondrial bioenergetic function by hydrogen sulfide. Part II. Pathophysiological and therapeutic aspects. *Br. J. Pharmacol.* **2014**, *171*, 2123−2146.

(17) Paul, B. D.; Snyder, S. H. Modes of physiologic H_2S signaling in the brain and peripheral tissues. *Antioxid. Redox Signaling* **2015**, *22*, 411−423.

(18) Feng, X.; Zhang, T.; Liu, J.-T.; Miao, J.-Y.; Zhao, B.-X. A new ratiometric fluorescent probe for rapid, sensitive and selective detection of endogenous hydrogen sulfide in mitochondria. *Chem. Commun.* **2016**, *52*, 3131−3134.

(19) Lin, V. S.; Chen, W.; Xian, M.; Chang, C. J. Chemical probes for molecular imaging and detection of hydrogen sulfide and reactive sulfur species in biological systems. *Chem. Soc. Rev.* **2015**, *44*, 4596−4618.

(20) Thorson, M. K.; Majtan, T.; Kraus, J. P.; Barrios, A. M. Identification of cystathionine β-synthase inhibitors using a hydrogen sulfide selective probe. *Angew. Chem., Int. Ed.* **2013**, *52*, 4641−4644.

(21) Liu, C.; Peng, B.; Li, S.; Park, C.-M.; Whorton, A. R.; Xian, M. Reaction based fluorescent probes for hydrogen sulfide. *Org. Lett.* **2012**, *14*, 2184−2187.

(22) Lin, V. S.; Chang, C. J. Fluorescent probes for sensing and imaging biological hydrogen sulfide. *Curr. Opin. Chem. Biol.* **2012**, *16*, 595−601.

(23) Qian, Y.; Karpus, J.; Kabil, O.; Zhang, S.-Y.; Zhu, H.-L.; Banerjee, R.; Zhao, J.; He, C. Selective fluorescent probes for live-cell monitoring of sulphide. *Nat. Commun.* **2011**, *2*, 495.

(24) Liu, C.; Pan, J.; Li, S.; Zhao, Y.; Wu, L. Y.; Berkman, C. E.; Whorton, A. R.; Xian, M. Capture and visualization of hydrogen sulfide via a fluorescent probe. *Angew. Chem., Int. Ed.* **2011**, *50*, 10327−10329.

(25) Lippert, A. R.; New, E. J.; Chang, C. J. Reaction-based fluorescent probes for selective imaging of hydrogen sulfide in living cells. *J. Am. Chem. Soc.* **2011**, *133*, 10078−10080.

(26) Taoka, S.; Lepore, B. W.; Kabil, Ö.; Ojha, S.; Ringe, D.; Banerjee, R. Human cystathionine β-synthase is a heme sensor protein. Evidence that the redox sensor is heme and not the vicinal cysteines in the CXXC motif seen in the crystal structure of the truncated enzyme. *Biochemistry* **2002**, *41*, 10454−10461.

(27) Kabil, O.; Vitvitsky, V.; Xie, P.; Banerjee, R. The quantitative significance of the transsulfuration enzymes for H_2S production in murine tissues. *Antioxid. Redox Signaling* **2011**, *15*, 363−372.

(28) Wintner, E. A.; Deckwerth, T. L.; Langston, W.; Bengtsson, A.; Leviten, D.; Hill, P.; Insko, M. A.; Dumpit, R.; VandenEkart, E.; Toombs, C. F.; Szabo, C. A monobromobimane-based assay to measure the pharmacokinetic profile of reactive sulphide species in blood. *Br. J. Pharmacol.* **2010**, *160*, 941−957.

(29) Mustafa, A. K.; Gadalla, M. M.; Sen, N.; Kim, S.; Mu, W.; Gazi, S. K.; Barrow, R. K.; Yang, G.; Wang, R.; Snyder, S. H. H_2S signals through protein S-sulfhydration. *Sci. Signaling* **2009**, *2*, ra72.

(30) Whiteman, M.; Li, L.; Rose, P.; Tan, C.-H.; Parkinson, D. B.; Moore, P. K. The effect of hydrogen sulfide donors on lipopolysaccharide-induced formation of inflammatory mediators in macrophages. *Antioxid. Redox Signaling* **2010**, *12*, 1147−1154.

(31) Abe, K.; Kimura, H. The possible role of hydrogen sulfide as an endogenous neuromodulator. *J. Neurosci.* **1996**, *16*, 1066−1071.

(32) Kimura, H. Hydrogen sulfide induces cyclic AMP and modulates the NMDA receptor. *Biochem. Biophys. Res. Commun.* **2000**, *267*, 129−33.

(33) Wong, P. T.; Qu, K.; Chimon, G. N.; Seah, A. B. H.; Chang, H. M.; Wong, M. C.; Ng, Y.-K.; Rumpel, H.; Halliwell, B.; Chen, C. P. High plasma cyst(e)ine level may indicate poor clinical outcome in patients with acute stroke: Possible involvement of hydrogen sulfide. *J. Neuropathol. Exp. Neurol.* **2006**, *65*, 109−115.

(34) Chan, S. J.; Chai, C.; Lim, T. W.; Yamamoto, M.; Lo, E. H.; Lai, M. K. P.; Wong, P. T. H. Cystathionine β-synthase inhibition is a potential therapeutic approach to treatment of ischemic injury. *ASN Neuro* **2015**, *7*, 1759091415578711.10.1177/1759091415578711

DOI: 10.1021/acscentsci.6b00019
ACS Cent. Sci. 2016, 2, 242−252

(35) Zhao, H.; Chan, S.-J.; Ng, Y.-K.; Wong, P. T. H. Brain 3-mercaptopyruvate sulfurtransferase (3MST): Cellular localization and downregulation after acute stroke. *PLoS One* **2013**, *8*, e67322.
(36) Panigrahi, K.; Applegate, G. A.; Malik, G.; Berkowitz, D. B. Combining a *Clostridial* enzyme exhibiting unusual active site plasticity with a remarkably facile sigmatropic rearrangement: Rapid, stereocontrolled entry into densely functionalized fluorinated phosphonates for chemical biology. *J. Am. Chem. Soc.* **2015**, *137*, 3600−3609.
(37) Karukurichi, K. R.; Fei, X.; Swyka, R. A.; Broussy, S.; Shen, W.; Dey, S.; Roy, S. K.; Berkowitz, D. B. Mini-ISES identifies promising carbafructopyranose-based salens for asymmetric catalysis: Tuning ligand shape via the anomeric effect. *Sci. Adv.* **2015**, *1*, e1500066.
(38) Karukurichi, K. R.; de la Salud-Bea, R.; Jahng, W. J.; Berkowitz, D. B. Examination of the new α-(2′Z-fluoro) vinyl trigger with lysine decarboxylase: The absolute stereochemistry dictates the reaction course. *J. Am. Chem. Soc.* **2007**, *129*, 258−259.
(39) Fei, X.; Connelly, C. M.; MacDonald, R. G.; Berkowitz, D. B. A set of phosphatase-inert "molecular rulers" to probe for bivalent mannose 6-phosphate ligand-receptor interactions. *Bioorg. Med. Chem. Lett.* **2008**, *18*, 3085−3089.
(40) Berkowitz, D. B.; Charette, B. D.; Karukurichi, K. R.; McFadden, J. M. α-Vinylic amino acids: Occurrence, asymmetric synthesis, and biochemical mechanisms. *Tetrahedron: Asymmetry* **2006**, *17*, 869−882.
(41) Berkowitz, D. B.; de la Salud-Bea, R.; Jahng, W.-J. Synthesis of quaternary amino acids bearing a (2′Z)-fluorovinyl α-branch: Potential PLP enzyme inactivators. *Org. Lett.* **2004**, *6*, 1821−1824.
(42) Berkowitz, D. B.; McFadden, J. M.; Chisowa, E.; Semerad, C. L. Organoselenium-based entry into versatile, α-(2-tributylstannyl)vinyl amino acids in scalemic form: A new route to vinyl stannanes. *J. Am. Chem. Soc.* **2000**, *122*, 11031−11032.
(43) Berkowitz, D. B.; Smith, M. K. A convenient synthesis of L-α-vinylglycine from L-homoserine lactone. *Synthesis* **1996**, *1996*, 39−41.
(44) Berkowitz, D. B.; Jahng, W.-J.; Pedersen, M. L. α-Vinyllysine and α-vinylarginine are time-dependent inhibitors of their cognate decarboxylases. *Bioorg. Med. Chem. Lett.* **1996**, *6*, 2151−2156.
(45) Tan, B. H.; Wong, P. T.; Bian, J. S. Hydrogen sulfide: A novel signaling molecule in the central nervous system. *Neurochem. Int.* **2010**, *56*, 3−10.
(46) Aitken, S. M.; Kirsch, J. F. Kinetics of the yeast cystathionine β-synthase forward and reverse reactions: Continuous assays and the equilibrium constant for the reaction. *Biochemistry* **2003**, *42*, 571−578.
(47) Lee, H.-K.; Bang, K.-T.; Hess, A.; Grubbs, R. H.; Choi, T.-L. Multiple olefin metathesis polymerization that combines all three olefin metathesis transformations: Ring-opening, ring-closing, and cross metathesis. *J. Am. Chem. Soc.* **2015**, *137*, 9262−9265.
(48) Hilinski, G. J.; Kim, Y.-W.; Hong, J.; Kutchukian, P. S.; Crenshaw, C. M.; Berkovitch, S. S.; Chang, A.; Ham, S.; Verdine, G. L. Stitched α-helical peptides via bis ring-closing metathesis. *J. Am. Chem. Soc.* **2014**, *136*, 12314−12322.
(49) Evande, R.; Ojha, S.; Banerjee, R. Visualization of PLP-bound intermediates in hemeless variants of human cystathionine β-synthase: Evidence that lysine 119 is a general base. *Arch. Biochem. Biophys.* **2004**, *427*, 188−196.
(50) Brooks, D.; Agid, Y.; Eggert, K.; Widner, H.; Ostergaard, K.; Holopainen, A. Treatment of end-of-dose wearing-off in Parkinson's disease: Stalevo (levodopa/carbidopa/entacapone) and levodopa/DDCI given in combination with comtess/comtan (entacapone) provide equivalent improvements in symptom control superior to that of traditional levodopa/DDCI treatment. *Eur. Neurol.* **2005**, *53*, 197−202.
(51) Burkhard, P.; Dominici, P.; Borri-Voltattorni, C.; Jansonius, J. N.; Malashkevich, V. N. Structural insight into Parkinson's disease treatment from drug-inhibited DOPA decarboxylase. *Nat. Struct. Biol.* **2001**, *8*, 963−967.
(52) Borri-Voltattorni, C.; Minelli, A.; Borri, P. Interaction of L-α-methyl-α-hydrazino-3,4-dihydroxyphenylpropionic acid with DOPA-decarboxylase from pig kidney. *FEBS Lett.* **1977**, *75*, 277−280.
(53) Stipanuk, M. H.; Ueki, I. Dealing with methionine/homocysteine sulfur: Cysteine metabolism to taurine and inorganic sulfur. *J. Inherited Metab. Dis.* **2011**, *34*, 17−32.
(54) Qu, K.; Chen, C. P.; Halliwell, B.; Moore, P. K.; Wong, P. T. Hydrogen sulfide is a mediator of cerebral ischemic damage. *Stroke* **2006**, *37*, 889−93.
(55) Whiteman, M.; Li, L.; Rose, P.; Tan, C.-H.; Parkinson, D. B.; Moore, P. K. The effect of hydrogen sulfide donors on lipopolysaccharide-induced formation of inflammatory mediators in macrophages. *Antioxid. Redox Signaling* **2010**, *12*, 1147−1154.
(56) Ekins, S.; Litterman, N. K.; Lipinski, C. A.; Bunin, B. A. Thermodynamic proxies to compensate for biases in drug discovery methods. *Pharm. Res.* **2016**, *33*, 194−205.
(57) Lipinski, C. A. Lead- and drug-like compounds: The rule-of-five revolution. *Drug Discovery Today: Technol.* **2004**, *1*, 337−341.
(58) Lipinski, C.; Hopkins, A. Navigating chemical space for biology and medicine. *Nature* **2004**, *432*, 855−861.

DOI: 10.1021/acscentsci.6b00019
ACS Cent. Sci. 2016, 2, 242−252